Applied Energy 202 (2017) 66–77

Contents lists available at ScienceDirect

Applied Energy

journal homepage: www.elsevier.com/locate/apenergy

Techno-economic optimization of hybrid photovoltaic/wind generation together with energy storage system in a stand-alone micro-grid subjected to demand response

Mohammad Hossein Amrollahi *, Seyyed Mohammad Taghi Bathaee

Department of Electrical Engineering, K.N. Toosi University of Technology, P.O. Box 16315-1355, Tehran, Iran

HIGHLIGHTS

- Ability of DR for component size optimization of a stand-alone micro-grid was examined.
- DR is implemented by reducing or eliminating the mismatch between the generation and consumption profiles.
- DR utilization, reduce the number of batteries, inverters, photovoltaic cells, and total net present costs.
- DR implementation reduces the peak of consumed loads and increased the consumed load factor and correlation factor.

GRAPHICAL ABSTRACT

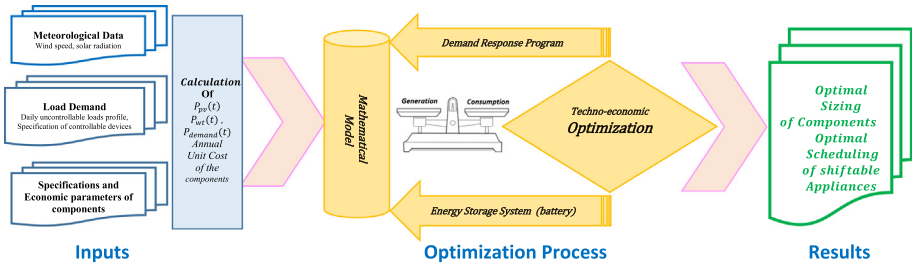

ARTICLE INFO

Article history:
Received 4 January 2017
Received in revised form 9 May 2017
Accepted 14 May 2017
Available online 25 May 2017

Keywords:
Size optimization
Micro-grid
Stand-alone
Mixed integer linear programming
Renewable resource energy
Demand response

ABSTRACT

Regarding the importance of supplying energy to regions that are far from power systems, this study is devoted to analyzing and modeling of a stand-alone micro-grid. In spite of many studies in the case of demand response programming for optimal management and operation cost reduction of the micro-grids, and regarding the importance of size optimization of micro-grids, this paper seeks to examine and investigate the ability of demand response programming in the case of component size optimization of a micro-grid. Due to deficiency or unavailability of dispatchable energy recourses, only the nondispatchable renewable energy resources (wind and solar energy) are considered to supply the required energy. Applied strategy for effective component size optimization as well as relevant costs reduction is implemented by reducing or eliminating the mismatch between the generation and consumption profiles by time shift and schedule of dispatchable loads. Furthermore, the effect of demand response utilization on loss of generated energy reduction is studied. The optimized results with and without demand response are extracted and compared to each other.

For each case, the optimum configuration was determined. Obtained results indicated that application of the demand response program, reduced the number of required batteries, the required inverter and photovoltaic cells capacity, and, consequently, the total net present costs. Furthermore, demand response implementation reduced the peak of consumed loads and increased the consumed load factor and correlation factor. The micro-grid components have been modeled mathematically within the framework of the mixed integer linear programming method. The optimization program has been performed by HOMER software together with GAMS software via the CPLEX solver.

* Corresponding author.
E-mail addresses: amrollahi_mh@yahoo.com (M.H. Amrollahi), bathaee@kntu.ac.ir (S.M.T. Bathaee).

http://dx.doi.org/10.1016/j.apenergy.2017.05.116
0306-2619/

1. Introduction

Nowadays, Interest in the use of renewable energy resources has been increased. This is due to rising of energy demand, limited resources of fossil fuels, energy market instability, as well as environmental threats on the one hand, and the free availability and limitlessness of renewable energy resources on the other hand. Moreover, the need to supply energy to remote regions from power distribution networks has further increased the importance of on-site renewable energy generation systems [1].

In the recent years, increased interest in the use of small-scale hybrid energy sources in electricity distribution networks has led to the appearance of smart micro-grids (MGs).

Wind and solar energy are considered as major renewable resources [2]. The amount of energy generated by these resources varies over time and does not usually match the consumption profile. This mismatch necessitates the use of batteries in an off-grid system. Also, if photo-voltaic (PV) systems or wind turbines (WT) are used separately, system size and investment cost will increase. Hybrid use of these sources can improve system reliability, performance, decrease generation fluctuations, investment costs, and the size of the storage system [3,4].

Notable studies have addressed the optimal design of hybrid power generation systems in micro-grids. In [5], Multi-objective Genetic Algorithms are used to optimize three stand-alone hydrogen storage systems. Application of meta-heuristic algorithms to optimize the size of hybrid systems has been reported in Refs. [6–8].

Technological development in the field of renewable resources makes these resources more usable for supplying power to small and remote sites. Numerous plans have been reported to meet the whole energy demand of off-grid systems using renewable energy resources and storage systems [9]. Panayiotou et al. [10] designed and employed an optimal standalone PV system and a standalone hybrid PV-WT system in Nicosia, Cyprus and Nice, France. Enevoldsen and Sovacool [11] examined the feasibility of implementing a standalone hybrid system (renewable energy only) in one of the Faroe's Islands. In Ref. [12], a storage system was used to increase reliability in an isolated micro-grid. In this study, various methods and tools for optimizing the design and selecting the components of a wide range of isolated micro-grids were examined. Zakeri and Syri [13] designed a standalone system equipped with a storage system to moderate the effects caused by the varying nature of energy supply/demand.

Considerable researches have been conducted in the case of size optimization of stand-alone micro-grids [14–16]. In Ref. [17], the metaheuristic method has been applied for the size optimization of the battery energy storage system in the hybrid power systems. In Ref. [8], colony optimization method has been implemented for size optimization renewable energy. Fadaee et al. [18] thoroughly examined the different methods for optimizing the size of hybrid renewable energy systems. In Ref. [19], a new formulation for optimizing the design of a photovoltaic (PV)-wind hybrid energy home system, incorporating a storage battery, was developed, using genetic algorithm. In Ref. [20], the capacity of an isolated micro-grid (PV/wind/battery bank) was optimized using iterative methods. In Ref. [21] size optimization of a micro-grid evolutionary algorithm was accomplished. In Ref. [22], the techno-economical optimization of an isolated system (PV/wind/diesel/battery) was addressed. This optimization was based on total unsupplied energy, total net present cost, and energy generation cost. In [23], size of an isolated system (PV/wind/diesel/battery) were minimized using harmony search algorithm. Mukhtaruddin et al. [24] optimized an autonomous hybrid system using iterative-Pareto-fuzzy methods. In Ref. [25] size optimization of a biomass-based PV power plant to supply the electrical power was done.

From previous studies, it has been found that a considerable amount of works have been performed on size optimization of micro-grids without DR programing.

In on-grid systems, demand response (DR) is often used to reduce operating costs. DR involves a change in consumption pattern in response to a change in electricity price over time or to cost incentives aimed at reducing consumption or shifting it to another time during hours when the market price of electricity is high or system reliability is in danger [26–29].

Recently, many studies have addressed the DR strategy for optimum power management in on-grid networks [30–33]. In Ref. [34] a new approach for solving the multi-area electricity resource allocation problem with considering both intermittent renewables and DR was proposed. Babonneau et al. introduced a linear programming framework to model distributed generation, flexible loads and distributed energy resources [35]. Tsui and Chan [36] proposed a method of minimizing electricity consumption cost using price-based DR for optimum operation of appliances in a smart home. Li and Hong [37] implemented a DR strategy for a smart home based on user-expected price with the aim of reducing total electricity cost. Yan et al. presented a novel demand response estimation framework for residential and commercial buildings using a combination of energy plus and two-state models for thermostatically controlled loads [38]. In Ref. [39] the promotion impact of demand response on distributed PV penetration was investigated. The DR strategy implemented in the study involved charging the electricity storage system (ESS) during off-peak times and discharging it during peak times. Previous studies are used DR only for optimal management and operation cost reduction without component size optimization.

To the best knowledge of the authors, no study has been done in the case of examining DR ability for size optimization.

Regarding the importance of size optimization of micro-grid, this paper seeks to examine the energy generation in a stand-alone micro-grid using DR programing. Due to deficiency or unavailability of dispatchable energy recourses, in the present study, only the available nondispatchable renewable energy resources (wind and solar energy) are considered to supply the desired energy (it must be noted that power management with nondispatchable energy recourses is more complicated than dispatchable ones). For the realistic modeling, consumed loads were considered as statistical normal distribution with mix of hourly and daily variation of loads. The studied micro-grid is a forestry camp, located in the northwest of Iran at longitude of $45^{\circ}, 5'$ and latitude of $37^{\circ}, 2'$. Consumed loads comprise dispatchable and nondispatchable loads. Applied strategy for effective component size optimization is implemented by reducing or eliminating the mismatch between the generation and consumption profiles by time shifting and schedule of dispatchable loads. In addition, the effect of applying this program on reducing the loss of generated energy is studied. Finally, the obtained optimization results with and without DR are compared to each other. The micro-grid components have been modeled mathematically within the framework of the mixed integer linear programming method. The applied software for modeling, simulating, and optimizing the studied micro-grid are GAMS and HOMER.

2. Model of the hybrid micro-grid system

Fig. 1 shows a schematic view of the studied isolated micro-grid. In this micro-grid, energy is generated using PV and WT. As shown in this figure, the micro-grid has an energy storage system (battery) to store energy generated in excess of consumption. Furthermore, the micro-grid has a smart system to manage

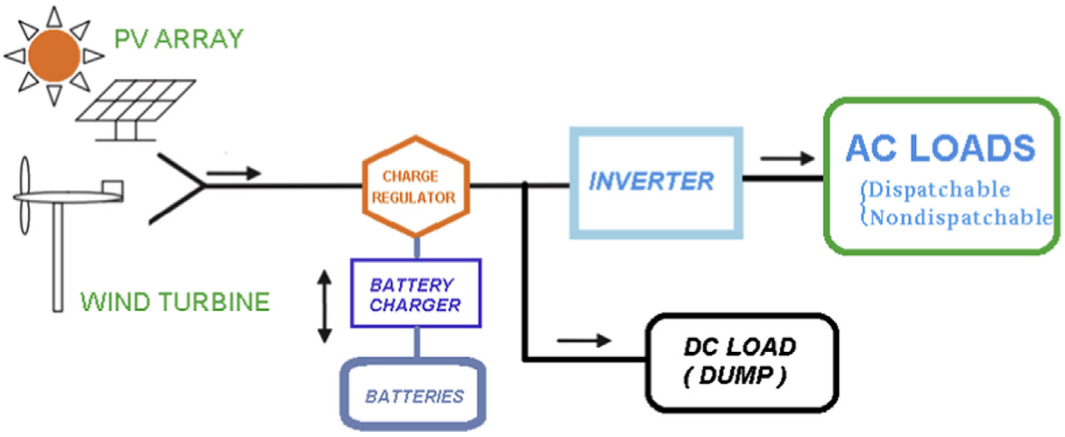

Fig. 1. Schematic of the PV/WT/battery-based hybrid system.

dispatchable loads. The smart system uses DR to reduce or eliminate the mismatch between the generation and consumption profiles. The dump load is used to dissipate power generated in excess of consumption and storage. The characteristics and equations related to each of the above components are given in the following sections.

3. Mathematical model for micro-grid components

The issue of determining the size of components for the studied micro-grid is mathematically formulated using mixed-integer linear programming (MILP).

The objective is to minimize the total life cycle cost of the micro-grid. In this optimization, scheduling the operation of dispatchable components was given particular attention. The decision variables are the capacity of the renewable solar and wind sources, the capacity of the ESS, the scheduling of ESS charge/discharge, operation times for dispatchable loads within the specified time window, and the amount of undistributed and unsupplied energy. The constraints of the issue include the operational and physical limitations of the components, energy balancing, constraints of generation sources, equipment capacity, and ESS constraints.

List of the components used in the MILP model are presented in the following.

3.1. Solar panel (photo-voltaic system)

A solar panel directly converts sunlight into electricity. The output DC power of the PV panel ($P_{PV}(t)$) depends on solar radiant intensity, absorption capacity, panel area, and cell temperature, and is described by Eq. (1) [40,41].

$$P_{PV}(t) = \frac{G_t(t)}{1000} \times P_{pv-rated} \times \eta_{pv} \times [1 - \beta_T(T_C - T_{C,STC})] \quad (1)$$

where $G_t(t)$ (w/m^2). the radiant power incident perpendicular to the surface of the array, $P_{pv-rated}$ is the nominal power of the panel under standard test conditions (STC), η_{pv} is the power reduction factor of photo-voltaic panels (%), $T_{C,STC}$ is cell temperature under STC, β_T is the PV temperature coefficient, and T_C is cell temperature under operating condition, which is given by:

$$T_C = T_{amb} + (NOCT - 20) \times \frac{G_t(t)}{800} \quad (2)$$

where $NOCT$ is normal operation cell temperature and T_{amb} is ambient temperature [42].

3.2. Wind turbine

The output power of a wind turbine ($P_{WT}(t)$) is a function of the wind speed at turbine hub altitude, as described by Eq. (3):

$$P_{WT}(t) = \begin{cases} 0, & v \leqslant v_{cut-in} \text{ or } v \geqslant v_{cut-out} \\ P_r\left(\frac{v^3 - v_{cut-in}^3}{v_r^3 - v_{cut-in}^3}\right), & v_{cut-in} < v \leqslant v_r \\ P_r, & v_r < v \leqslant v_{cut-out} \end{cases} \quad (3)$$

In this relation, v (m/s), v_r, v_{cut-in}, and $v_{cut-out}$ represent, respectively, the wind speed at turbine hub altitude, nominal speed, cut-in speed, and cut-out speed for the wind turbine. P_r represents the output power at rated speed (v_r). Fig. 2 shows output power versus wind speed for a wind turbine.

The wind speed at turbine hub altitude can be obtained as a function of the reference speed using Eq. (4),

$$v_w^h = v_w^{ref} \times \left(\frac{h}{h_{ref}}\right)^{\gamma} \quad (4)$$

where h is turbine hub altitude, and v_w^{ref} is the reference speed at the height h_{ref}. Gamma (γ) is a value ranging between 0.1 (for flat terrain) and 0.25 (for forested and tree-covered terrain). In this paper, the site under study is located on non-flat, tree-covered terrain. For this type of terrain, γ is assumed to be 0.25 [4,43,44].

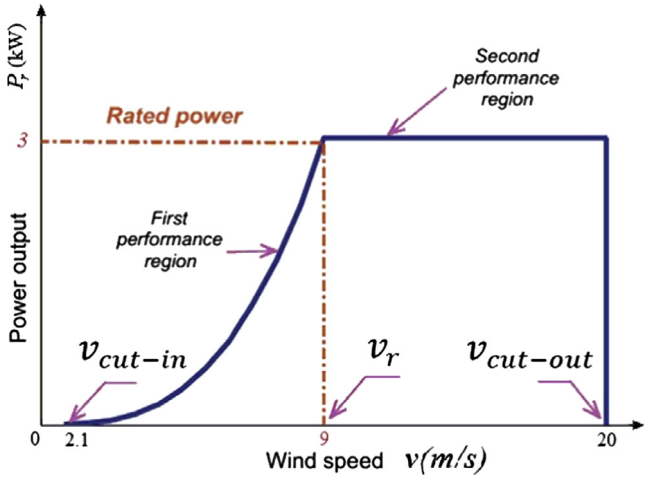

Fig. 2. Power curve characteristics of wind turbine [22].

3.3. Energy storage system (battery)

Energy storage is used to simultaneous balance of supply and demand. In a micro-grid, a battery bank can be used as a storage system. It can be charged or discharged depending on the generation power and consumption power. The input power of the batteries can be either positive or negative depending on whether the battery bank is being charged or discharged (Eq. (5)).

$$P_B(t) = P_{WT}(t) + P_{PV}(t) - P_L(t)/\eta_{inv} \tag{5}$$

In the above relation, P_L is total consumption loads at the time t and η_{inv} is inverter efficiency.

If $P_B = 0$, then the battery bank is neither being charged nor being discharged.

If $P_B > 0$, then the battery bank is being charged due to a surplus of generated power in the micro-grid. In this situation, the new state of charge for the battery bank is given by Eq. (6).

$$SOC_B(t) = SOC_B(t-1) \times (1-\sigma) + [P_{WT}(t) + P_{PV}(t) - P_L(t)/\eta_{inv}] \times \eta_b \tag{6}$$

If $P_B < 0$, then the battery bank is being discharged due to a shortage of generated power in the micro grid. In this situation, the new state of charge for the battery bank is given by Eq. (7).

$$SOC_B(t) = SOC_B(t-1) \times (1-\sigma) - [P_{WT}(t) + P_{PV}(t) - P_L(t)/\eta_{inv}] \times \eta_b \tag{7}$$

In the above relations, $SOC_B(t)$ and $SOC_B(t-1)$. are the battery bank state of charge at the times t and $t-1$, respectively, σ is the self-discharge of the batteries, and η_b is the efficiency of the batteries.

To prevent energy accumulation in the ESS, the initial state of charge at the beginning and end of each planning period should be equal (Eq. (8)).

$$SOC(t=0) = SOC(t=T) \tag{8}$$

Unlike most similar studies, in this paper, the optimized initial state of charge is obtained using the optimization model.

To prevent a reduction in the useful life of each battery, the constraint in Eq. (9) is imposed for charge and discharge.

$$\begin{aligned} &E_{batmin} \leqslant E_{bat}(t) \leqslant E_{batmax} \\ &SOC_{min} = N_{bat} \times E_{batmin} \\ &SOC_{max} = N_{bat} \times E_{batmax} \end{aligned} \tag{9}$$

where $E_{bat}(t)$ represents the energy stored in each battery, E_{batmax}, E_{batmin}, SOC_{max} and SOC_{min} represent, respectively, the maximum and minimum allowable amounts of energy for storage in each battery and battery bank, and N_{bat} is the number of batteries, which the maximum and minimum allowable capacity level of each battery are related to each other by Eq. (10) [45].

$$E_{batmin} = (1 - DOD) \times E_{batmax} \tag{10}$$

where DOD is the allowable depth of discharge (DOD) for each battery.

Since simultaneous charge and discharge of the battery bank is not possible, the constraint in (11) is imposed on the linear modeling.

$$\begin{aligned} &PEES_{ch}(t) \leqslant M \times IESS_{ch}(t), \ \forall t \\ &PEES_{dis}(t) \leqslant M \times IESS_{dis}(t), \ \forall t \\ &IESS_{ch}(t) + IESS_{dis}(t) \leqslant 1, \ \forall t \end{aligned} \tag{11}$$

In the above relations, the binary variables $IESS_{ch}(t)$ and $IESS_{dis}(t)$ represent, respectively, the "charge" and "discharge" status of the battery bank at the time t; $PEES_{ch}(t)$ and $PEES_{dis}(t)$ represent, respectively, the charge power and discharge power of the battery bank at the time t. Based on linear programing [46], for satisfying constraints of Eq. (11) M is considered as a positive large number that must be greater than the capacity of the batteries. This assumption indicates that batteries can't be charged and discharged simultaneously. In this paper M is considered as 200.

To prevent damage to the batteries, the charge rate and the discharge rate of each battery must not exceed the limit specified by the manufacturer (Eq. (12)).

$$\begin{aligned} &E_{bat}(t) - E_{bat}(t-1) \leqslant IESS_{ch}(t) \times RESS_{ch}, \ \forall t \\ &E_{bat}(t-1) - E_{bat}(t) \leqslant IESS_{dis}(t) \times RESS_{dis}, \ \forall t \end{aligned} \tag{12}$$

In these relations, $RESS_{ch}$ and $RESS_{dis}$ are the charge rate and the discharge rate of each battery, respectively. If a battery is to be discharged during the interval t, then it needs to have been sufficiently charged during previous intervals.

3.4. Demand response program

Since the whole energy demand of the micro grid is to be provided using renewable energy resources, the flexibility of power generation is low. Therefore, in order to balance generation and consumption, responsive loads can be controlled, through which the low generation flexibility can be compensated for to a considerable extent.

In this paper, a new application of DR is presented. The operation of dispatchable loads is scheduled to reduce or eliminate the mismatch between the consumption and generation profiles through DR programing.

For each dispatchable load, the desired time range for the beginning and end of operation is specified by the consumer. Then, the optimum time for the operation of dispatchable loads within the specified interval is determined (Fig. 3).

If optimum operation is to be achieved for a dispatchable appliance k, it has to be ON during a certain time span ($span_k$) within its allowable time interval (Eq. (13)).

$$\sum_{t=EST_k}^{LFT_k} flag_k(t) = span_k, \ \forall k \tag{13}$$

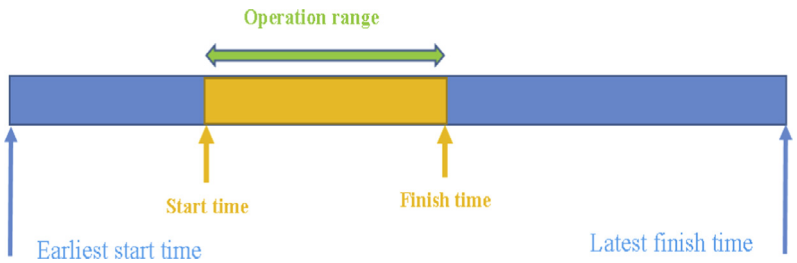

Fig. 3. Operation interval each device [47].

The binary variable $flag_k$ represents the ON/OFF status of the *kth* appliance. $flag_k = 1$ means that the appliance is ON during that interval, while $flag_k = 0$ means that it is OFF. $span_k$ indicates operation range of *kth* appliance (see Fig. 3). EST_k is the earliest start time and LFT_k is the latest finish time. To achieve continuous operation for a dispatchable appliance during consecutive time intervals, the constraint in (14) is imposed,

$$\sum_{t=rang}^{rang+span_k-1} flag_k(t) \geqslant span_k \times ON_k, \forall rang \leqslant 96 - span_k + 1, \ \forall k \tag{14}$$

where the binary variable $ON_k(t)$ shows whether the appliance k is turned on during the time interval t. $ON_k(t) = 1$ means that the appliance k is turned on during the time interval t. Similarly, the binary variable $OFF_k(t)$ shows whether the appliance k is turned off during the time interval t. $OFF_k(t) = 1$ means that the appliance k is turned off during the time interval t. Eq. (15) describes the relationship between these two variables and appliance operation.

$$ON_k(t) - OFF_k(t) = flag_k(t) - flag_k(t-1), \ \forall t, \ \forall k \tag{15}$$

To prevent an appliance from being turned on and off simultaneously, the constraint in (16) is imposed.

$$ON_k(t) + OFF_k(t) \leqslant 1, \ \forall t, \ \forall k \tag{16}$$

3.5. Energy balancing

In order for a power system to be stable, total consumption power should be equal to total generation power. In other words, during each time period, the electric energy consumed by nondispatchable and dispatchable appliances plus the energy charged into the storage system should be equal to the energy supplied by PV and WT plus the energy discharged from the storage system. Perfect balancing during each time interval is not possible. This is due to the restriction on the charge and discharge rates of the storage system, the restriction on the capacity of dispatchable loads, and the uncontrollability of the amount of power generated by renewable energy sources. Therefore, to overcome this problem, a variable for consumption is added to the Eq. (17).

$$Pload_{ncl}(t) + Pload_{cl}(t) + PEES_{ch}(t) + Pload_{dump}(t) = P_{PV}(t) + P_{WT}(t) + PEES_{dis}(t), \ \forall t \tag{17}$$

where $Pload_{ncl}(t)$, $Pload_{cl}(t)$, $PEES_{ch}(t)$, $Pload_{dump}(t)$, and $PEES_{dis}(t)$ represent, nondispatchable loads, dispatchable loads, the batteries charge power, dump loads, and the batteries discharge power, respectively.

4. Costs of system components

The total cost of the k_{th} component in a hybrid system comprises the following elements: the initial cost of procurement, installation, and commissioning (IC_k), replacement cost (Rep_k), operation and maintenance cost ($O\&M_k$), and residual value (RV_k). The total cost (TUC_k) for the k_{th} component is given by Eq. (18).

$$TUC_k = IC_k + Rep_k + O\&M_k - RV_k \tag{18}$$

Time of allocation for each cost is as follows: initial cost (at the beginning of the project), replacement cost (at the end of the useful life of each component up to the end of the system lifetime), operation and maintenance cost (annually during the system lifetime), residual value (at the end of the system lifetime). In this paper, to economic evaluation of the system, the costs of components are calculated annually, as well as the net present value is calculated.

To convert the initial cost to annual cost, the capital recovery factor ($CRF(i,n)$) is used, as described by Eq. (19).

$$CRF(i,n) = \frac{i(1+i)^n}{(1+i)^n - 1} \tag{19}$$

where i is the interest rate, n is the system lifetime, and n_k is the lifetime of the k_{th} component. The annual initial cost of the k_{th} component is given by Eq. (20).

$$AIC_k = IC_k \times CRF(i,n) \tag{20}$$

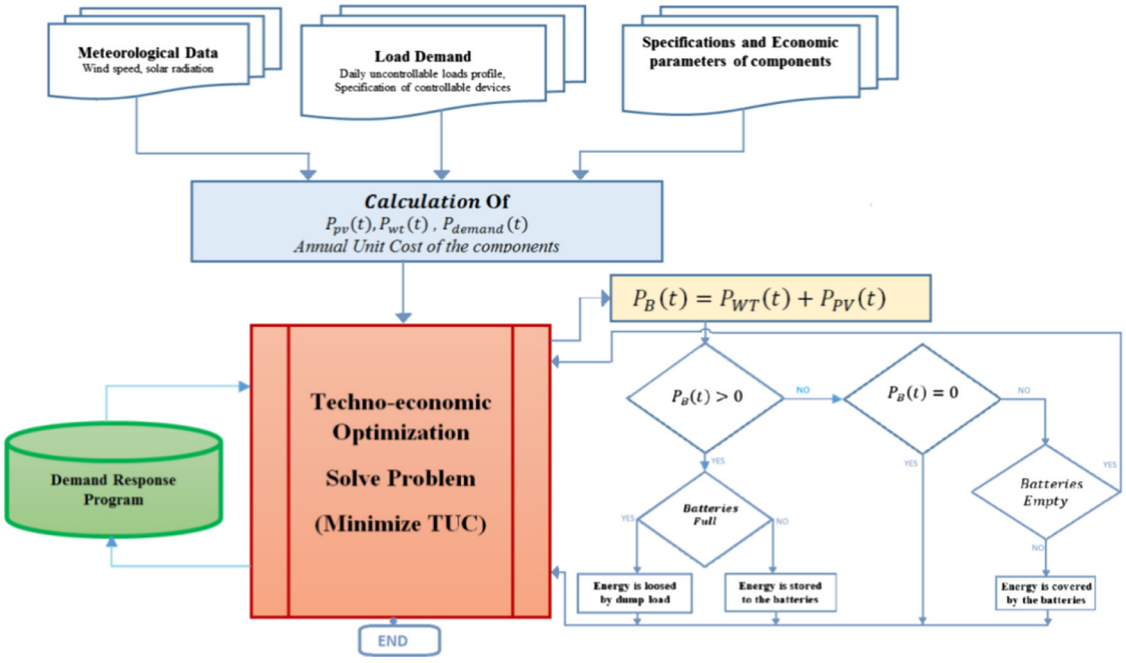

Fig. 4. schematic view of optimization procedure of the micro-grid.

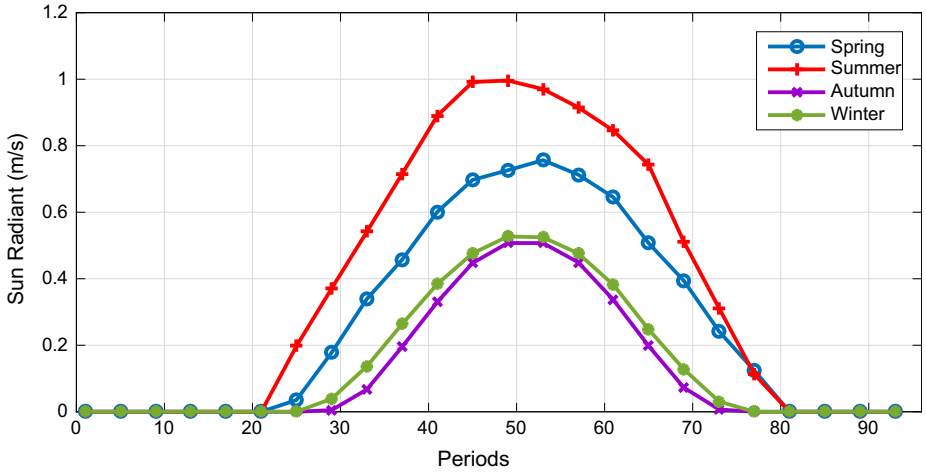

Fig. 5. Mean-hourly of sun radiant for seasons.

The annual replacement cost of the k_{th} component is given by Eq. (21).

$$A\,\mathrm{Rep}_k = \mathrm{Re}\; p_k \times \sum_{m=0}^{\left[\frac{n}{n_k}\right]-1} \frac{1}{(1+i)^{m\times n_k}} \tag{21}$$

The residual value (scrap value) of the k_{th} component is given by:

$$ARV_k = RV_k \times \sum_{m=1}^{\left[\frac{n}{n_k}\right]} \frac{1}{(1+i)^{m\times n_k}} \tag{22}$$

The annual unit cost of the components of the hybrid system can be obtained as:

$$ATUC_k = AIC_k + APep_k + O\&M_k - ARV_k \tag{23}$$

Therefore, the net present cost (NPC) of the k_{th} component is given by Eq. (24).

$$NPCU_k = ATUC_k / CRF(i,n) \tag{24}$$

5. Optimization problem

Optimization procedure consists of input data (such as meterology, loads, and specification and economic parameters of components) and is conceived as a MILP model that is performed by the EMS to jointly schedule appliances power consumption and the energy. The objective of minimizing the amount total net present cost of the micro-grid over its life time. Schematic view of this procedure is depicted in Fig. 4.

Electric appliances divided into two categories: (i) shiftable appliances (including Water electro-pump, Clothes dryer, Clothes washer, and Dish washer), which can be run at flexible time schedule in scope of a day (by energy management system (EMS)), or (ii) non-shiftable appliances, which are uncontrollable and cannot be scheduled.

5.1. Objective function

The objective function of the optimum design problem is the minimization of total net present cost of the micro-grid over its life time. The life time of the system is marked as 25 years that is equal to the longest lifespan of components. Total net present cost for the hybrid renewable energy system is as:

$$MinimizingTUC = \sum_{k=\{PV,WT,Batt,Inv\}} NPCU_k \times N_k \tag{25}$$

where $NPCU_k$ is the net present cost of the k_{th} component and N_k is the number/capacity of k_{th} component, and also N_{WT} and N_{Batt} are integer decision variables, and N_{PV} and N_{INVER} are continuous decision variables.

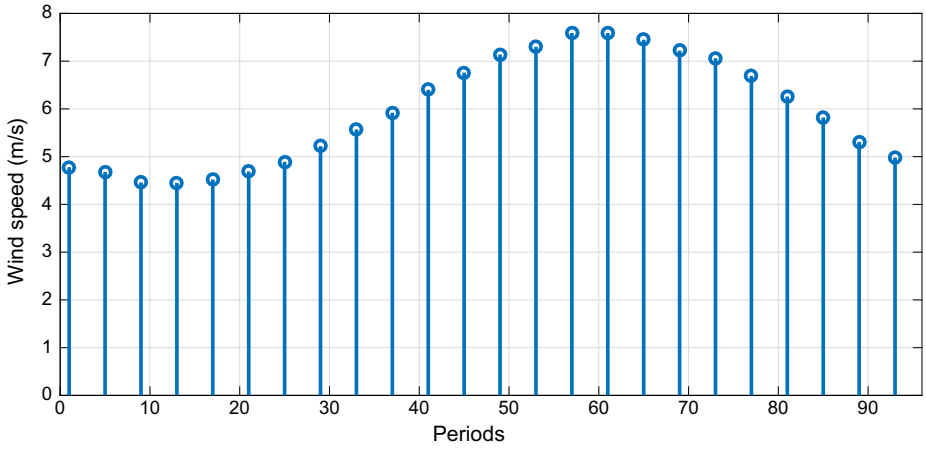

Fig. 6. Mean annually of wind speed for each hour.

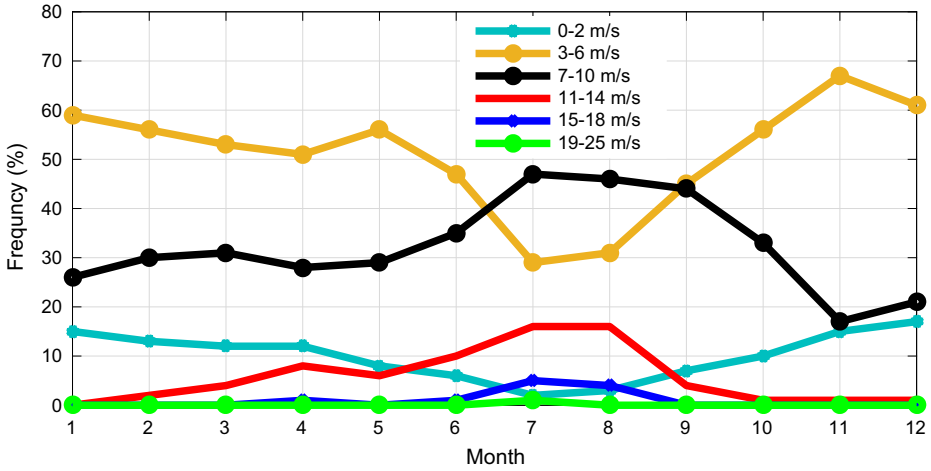

Fig. 7. Frequency distribution of wind speed for each month.

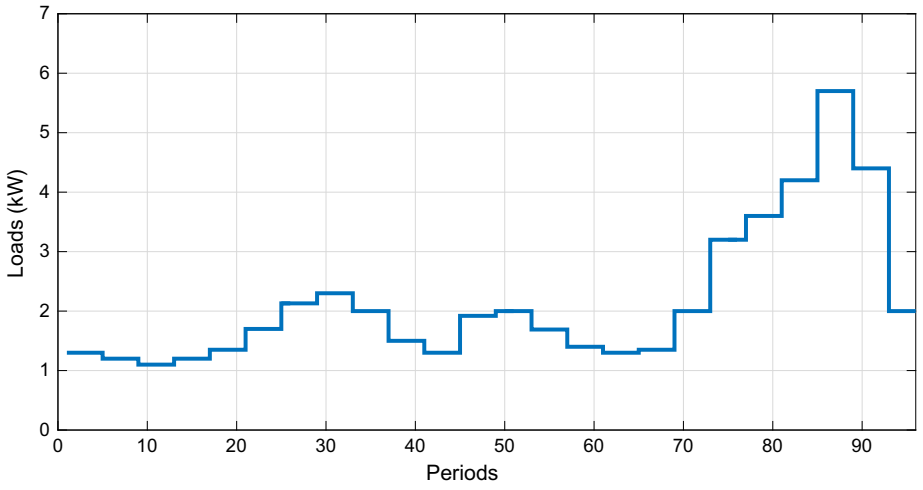

Fig. 8. Mean value of daily loads (power) profile.

5.2. Constraints

As explained before (Section 3), the constraints of the study comprise of physical constraints of micro-grid components, energy balance, reliability, and DR constraints.

In the present optimization, adequacy reliability is considered 100%, in other word loss of load expectation equals with zero.

DR interacts with the Energy Management System (EMS) to receive an optimal schedule for the shiftable loads. The output of the EMS is the optimized power profiles of the scheduled appliances.

6. Case study

In this section technical and economical specification of appliances and micro-grid components and relevant meteorology data are presented. Studied micro-grid is a forestry camp placed in north-west of Iran (with Long: 45°, 5′, Lat:37°2′ and Altitude: 1650 m). Proposed method for planning of the micro-grid is considered for 25 years of lifetime.

Required meteorology data's (wind speed and sun radiant) are provided from meteorology site (see Refs. [48,49]) and are presented in mean-hourly for seasons in Figs. 5–7.

Characteristics of mean value of consumed loads of the micro-grid for a one day is shown in Fig. 8.

As shown in this figure average of daily consumed energy and load (power) peak are 51.84 kW h and 5.7 kW respectively. Inherent of loads is statistical and should be considered in modeling process. With mix of hourly and daily variation of loads, a realistic model can be extracted. For this reason average of hourly loads is multiplied in perturbation coefficient as Eq. (26) [37].

$$k_{cv} = 1 + \delta_d + \delta_t \tag{26}$$

δ_d is a normal distribution with zero mean, which standard deviation of this distribution is in "daily variation percent". δ_t is a normal distribution with zero mean which standard deviation of this distribution is "hourly variation percent". For this study daily variation percent and hourly variation percent are assumed 20% and 15%, respectively. Fig. 9 shows a sample for such loads variation.

Time window for planning of controllable loads is 15 min. So one day has 96 time-window. Consumed loads of micro-grid is comprised four controllable appliances with total consumption of 3.95 kW h/days (about 7.5% of total consumed loads) and some unresponsive appliance with 47.89 kW h/days consumed. Input information of each dispatchable appliances are presented in Table 1.

Techno-economical specifications of micro-grid components are shown in Table 2. Also annual Unit Cost and net present cost of micro-grid components were calculated and presented in Table 3.

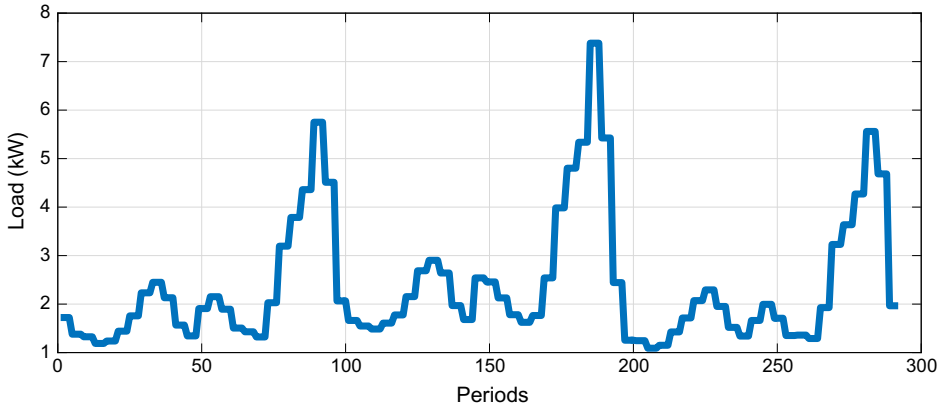

Fig. 9. Effects of hourly and daily loads changes in loads profile.

Table 1
Specification of dispatchable appliances.

Device	Consumed energy for an one day (kW h)	Performance duration (time interval)	Earliest start time	Latest finish time
Water electro-pump	2.00	8	30	90
Clothes dryer	0.9375	5	1	96
Clothes washer	0.750	6	35	56
Dish washer	0.2625	3	45	87

Table 2
Specifications of the micro-grid components and Economic indicators [50,44,51].

Specifications of the PV module		reference height (h_{ref})	10m
Rated capacity	1 kW	turbine hub height (h)	15m
Investment cost	2800$/unit	Gamma (γ)	0.25
Maintenance cost	5$/year	**Specifications of the Battery**	
Lift time (year)	25	Rated capacity	1.2kWh
reduction factor of panels (η_{PV})	85%	Investment cost	270$/unit
cell temperature under STC ($T_{c,STC}$)	25 °C	Replacement cost	250$/unit
PV temperature coefficient (β_T)	0.0045	Efficiency	80%
Normal operation cell temperature (NOCT)	55 °C	depth of discharge (DOD)	20%
Specifications of the Wind Turbine		self-discharge (σ)	0.002
Rated capacity	3 kW	Maintenance cost	5$/year
Investment cost	8000$/unit	Lift time (year)	5
Replacement cost	7000$/unit	**Specifications of the Inverter**	
Maintenance cost	250$/year	Rated capacity	1.0 kW
Lift time (year)	20	Investment cost	700$/unit
v_{cut-in}	2.1 (m/s)	Replacement cost	600$/unit
$v_{cut-out}$	20 (m/s)	Efficiency	95%
v_r	9 (m/s)	Lift time (year)	10
Economic indicators			
i (interest rate)		6%	
RV (Residual Value)		10% Investment cost	

Table 3
Annual unit cost and net present cost of micro-grid components.

Cost of unit component ($)	Photovoltaic cells	Wind turbine	Batteries bank	Inverter
Annual Unit Cost	222.9	893.7	62.6	82.7
Net Present Cost	2849.7	11424.9	890.2	1056.8

Table 4
Concise results of optimum size of the micro-grid components.

Item	Rated capacity	
	Optimal results With DR	Optimal results Without DR
Photovoltaic cells	16.7 kW	17 kW
Wind Turbine	9 kW	9 kW
battery bank	58 kW h	90 kW h
inverter	3.9 kW	6 kW

7. Simulation, results and discussion

In this paper, obtained results of size optimization of the micro-grid with and without DR implementation are presented. In current study, the issue is modeled as mixed integer linear programing. GAMS 23.6 software with CPIEX solver [52] along with HOMER [53], which is a useful software for programing of micro-grid are applied for size optimization.

Size optimization of the micro-grid is accomplished for 2 cases: with and without DR. Table 4 presents essence of size optimization results for these cases.

Consumed power is equal for two cases. Part of generated power is wasted in charge and discharge processes. Origin of this slight difference in the number of photovoltaic panels is this waste.

Table 5
Comparison of components and net present costs for two cases (with and without DR).

Net present cost ($)	Photovoltaic cells		Wind turbines		Batteries bank		Inverters		System	
	Without DR	With DR	Without DR	With DR	Without DR	With DR	Without DR	With DR	Without DR	With DR
Capital	47538.1	46699.2	24000.0	24000.0	24300.0	15660.0	4175.9	2714.3	100014.0	89073.5
Replacement	0.0	0.0	4634.2	4634.2	37655.3	24266.7	2425.8	1576.8	44715.3	30477.7
O&M	906.2	890.2	8006.1	8006.1	4803.7	3095.7	0.0	0.0	13716.0	11992.0
Residual value	0.0	0.0	2365.5	2365.5	0.0	0.0	261.3	169.8	2626.8	2535.3
Total	48444.2	47589.4	39005.8	39005.8	66758.9	43022.4	6863.0	4461.0	161071.9	134078.5

Table 6
Operation intervals for controllable appliances.

Water electro-pump	Clothes dryer	Washing machine	Dish washer
46–51	42–48	54–57	48–56

But as shown in this table, application of DR causes to considerable reduction of batteries and inventers capacity. This reduction has two reasons: firstly, due to approach of consumed loads profile and generated power profile; secondly, due to reduction of consumed loads peaks. Related results are presented in the continuation of paper.

Also, the net present cost of each component and the total net present cost of micro-grid are obtained and illustrated in Table 5. Implementation of the DR program led to significant reductions in the capacity number of components as well as the energy supply costs. As shown in this figure, DR program reduces the power storage system, the inventers, the PV panels and the total costs by 35%, 35.6%, 1.8% and 17.2%respectively.

It is expected that, running of the DR program cause to shift of controllable loads from intervals with shortfall generated power to intervals with surplus generated power, and as the consequence of this transformation, consumed and generated power profiles get closer to each other. The proposed scheduling DR program for controllable appliances is presented in Table 6.

Consumed loads profile without DR is presented in Fig. 10. For the case of DR implementation, consumed loads profile is obtained and presented in Fig. 10. As it can be seen in this figure, there is a significant increase in the consumed loads for this intervals 42–56. This increase is because of high power generation during this intervals. But a considerable reduction in consumption for 86–93 interval is observable, due to shortage of generated power. In fact, DR implementation provides the possibility of bringing the consumption and generation profiles closer together, through shifting of partly loads towards the intervals with surplus power generation.

It must be noted that the sum of areas under each diagrams (energies) given in figure are equal. In other words, application of the DR program does not remove any consumption loads, but just only changes consumption time. In general, the following equation can be presented for the consumption loads diagrams obtained with and without running the DR program.

$$\int_{t=0}^{t=T} P_{demand}(withDR)dt = \int_{t=0}^{t=T} P_{demand}(withoutDR)dt \tag{27}$$

In the specific condition, following equation is accurate for diagram of Fig. 10.

$$\int_{t=42}^{t=56} [P_{demand}(withDR) - P_{demand}(withoutDR)]dt = \int_{t=86}^{t=93} [P_{demand}(withoutDR) - P_{demand}(withDR)]dt \tag{28}$$

Load factor (LF) represents the smoothness of the consumption loads curve and is expressed as Eq. (29). This parameter is defined in the $0 \leqslant LF \leqslant 1$ range. For the ideal mode, LF is equal to unity, which indicating constant load consumption during the operation period. For constant power consumption during a specified period, increasing peak consumption loads causes LF to tend towards zero. Conversely, decreasing LF would increase the peak consumption loads that necessitating increase the capacity of power supply components. As a result of extend in the capacity of micro-grid components, the initial investment and operation costs would also raise.

$$LoadFactor = \left[\frac{\sum_{t=1}^{T} P_{Demand}(t)}{T \times \max(P_{Demand}(t))}\right] \tag{29}$$

As shown in Fig. 10, peak and LF are 3.6 kW and 0.60 for the case where DR is used and 5.7 kW and 0.38 for the case where DR is not used. Therefore, application of the DR program would cause a significant reduction (36.8%) in the peak load and a considerable increase (57.9%) in LF, and consequently leading to an increased smoothness of loads curve and a reduction in the

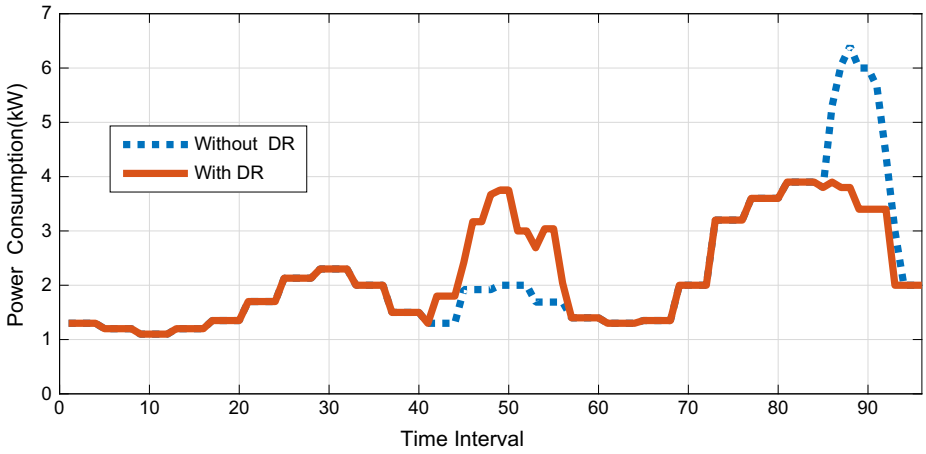

Fig. 10. Consumed loads profiles for a one day for two cases (with and without DR).

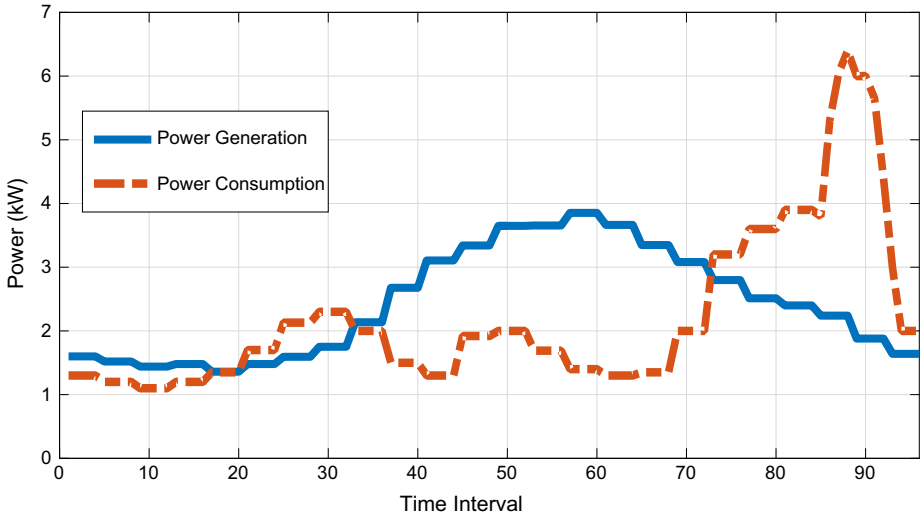

Fig. 11. Generated power and consumed loads profiles without DR application.

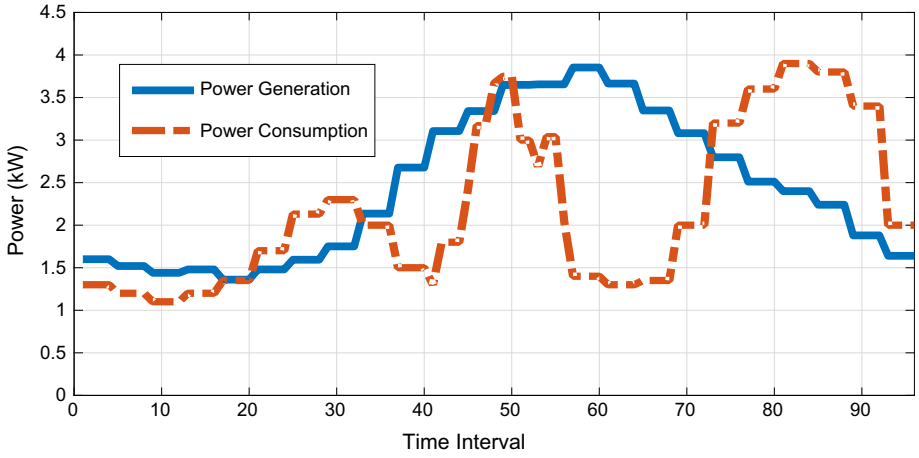

Fig. 12. Generated power and consumed loads profiles with DR application.

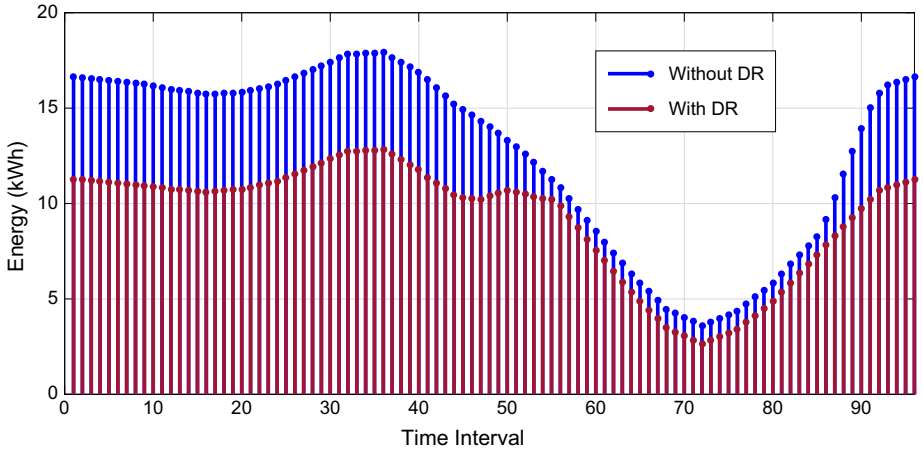

Fig.13. Charge and discharge states of batteries.

quantity of the required micro-grid components. This cost reduction represents only one of the several advantages of DR application, although the main purpose of the DR program is to produce closeness of power consumption and power generation profiles, and, if possible, to coincide the two profiles.Fig. 11 shows generated power and consumed loads profiles without DR and Fig. 12 shows generated power and consumed loads profiles with DR application.

Index of relative difference coefficient for evaluation of approach of generated power and consumed loads profiles is defined as Eq. (30).

$$DF = \frac{\sum_{t=1}^{T} |P_{Demand}(t) - [P_{PV}(t) + P_{WT}(t)]|}{\sum_{t=1}^{T} P_{Demand}(t)} \quad (30)$$

DF index for the cases of with and without DR are 0.406 and 0.551, respectively. Which indicates that, utilizing of DR cause to reduction of DF index and closeness of consumed and generated powers.

According to Figs. 11 and 12 DF indices for conditions of with and without DR application are 0.406 and 0.551 respectively. This indicates that applying of DR program causes to reduction of DF index by 26.3% and causes to approach of generated and consumed profiles. Furthermore, correlation factor of generated power and consumed loads for the cases of with and without DR are +0.2093 and −0.07813 respectively; that application of DR causes to increase of this factor by 368%.

Fig. 13 shows the stored energy profiles for the two mentioned cases (with and without DR). As shown in this figure, implementation of DR significantly reduced the stored energy. This can reduce purchase and maintenance costs associated with the storage system. Note that the stored energy in the case of applying DR is always less than or equal to the stored energy in the case of without applying DR that is Eq. (31).

$$P_{storage}(withDR) \leqslant P_{storage}(withoutDR), \ \forall t \quad (31)$$

Attention to Eq. (32) following inequality is correct for the total stored energy with period of a one day.

$$\int_{t=0}^{t=T} P_{storage}(withDR)dt \leqslant \int_{t=0}^{t=T} P_{storage}(withoutDR)dt \quad (32)$$

8. Conclusion

In spite of many studies in the case of DR programming for optimal management and operation cost reduction of the micro-grids, and attention to importance of size optimization of micro-grids, this paper was devoted to examine of ability of DR programming in the case of component size optimization of a micro-grid. Due to deficiency or unavailability of dispatchable energy recourses, only the nondispatchable renewable energy resources (wind and solar energy) were considered to supply the required energy.

For size optimization, DR scheduling program was employed to provide a better coincide between the generated power and consumed energy profiles and also to minimize the components size of micro-grid as well as the relevant costs.

The micro-grid components were mathematically modeled within the framework of the integer linear programming method. The optimum program for controllable appliances was performed by GAMS software via the CPLEX solver. And optimization results (using HOMER software) for two cases, with and without applying the DR program were extracted and compared with each other. For each case, the optimum configuration was determined. Obtained results indicated that application of the DR program, significantly reduced the number of required batteries by 35.6%, the inverter capacity by 35%, PV panels by 1.8% and, consequently, the net present costs by 17.1% (including investment, repair and maintenance, and replacement costs). As a result, compared to the case of without DR applying, the storage system, the inventers and the total costs were reduced by 35%, 35.6% and 17.2% respectively. Furthermore, DR implementation reduced the peak of consumed loads and DF index by 36.8% and 26.3% respectively. Also increased the consumed load factor and correlation factor by 57.9% and 368%, respectively.

This paper showed good ability of DR programming in the case of component size optimization of a stand-alone micro-grid for only 7.5% dispatchable loads. It is obvious that for higher percentage, ability of DR for size optimization increased.

Appendix A. Supplementary material

Supplementary data associated with this article can be found, in the online version, at http://dx.doi.org/10.1016/j.apenergy.2017.05.116.

References

[1] Mazandarani A, Mahlia TMI, Chong WT, Moghavvemi M. A review on the pattern of electricity generation and emission in Iran from 1967 to 2008. Renew Sustain Energy Rev 2010;14(7):1814–29.
[2] Erdinc O, Uzunoglu M. Optimum design of hybrid renewable energy systems: overview of different approaches. Renew Sustain Energy Rev 2012;16(3):1412–25.
[3] Wang Caisheng, Hashem Nehrir M. Power management of a stand-alone wind/photovoltaic/fuel cell energy system. IEEE Trans Energy Convers 2008;23(3):957–67.
[4] Yang Hongxing et al. Optimal sizing method for stand-alone hybrid solar–wind system with LPSP technology by using genetic algorithm. Solar Energy 2008;82(4):354–67.
[5] Brka A, Al-Abdeli YM, Kothapalli G. The interplay between renewables penetration, costing and emissions in the sizing of stand-alone hydrogen systems. Int J Hydrogen Energy 2015;40(1):125–35.
[6] Kaviani A Kashefi, Riahy GH, Kouhsari SHM. Optimal design of a reliable hydrogen-based stand-alone wind/PV generating system, considering component outages. Renewable Energy 2009;34(11):2380–90;
Maleki Akbar, Ameri Mehran, Keynia Farshid. Scrutiny of multifarious particle swarm optimization for finding the optimal size of a PV/wind/battery hybrid system. Renewable Energy 2015;80:552–63.
[7] Maleki Akbar, Pourfayaz Fathollah. Optimal sizing of autonomous hybrid photovoltaic/wind/battery power system with LPSP technology by using evolutionary algorithms. Solar Energy 2015;115:471–83.
[8] Fetanat Abdolvahhab, Khorasaninejad Ehsan. Size optimization for hybrid photovoltaic–wind energy system using ant colony optimization for continuous domains based integer programming. Appl Soft Comput 2015;31:196–209.
[9] Petruschke P, Gasparovic G, Voll P, Krajačić G, Duić N, Bardow A. A hybrid approach for the efficient synthesis of renewable energy systems. Appl Energy 2014;135:625–33.
[10] Panayiotou G, Kalogirou S, Tassou S. Design and simulation of a PV and a PV-Wind standalone energy system to power a household application. Renewable Energy 2012;37:355–63.
[11] Enevoldsen P, Sovacool BK. Integrating power systems for remote island energy supply: lessons from Mykines, Faroe Islands. Renewable Energy 2016;85:642–8.
[12] Mahesh A, Sandhu KS. Hybrid wind/photovoltaic energy system developments: Critical review and findings. Renew Sustain Energy Rev 2015;52:1135–47.
[13] Zakeri B, Syri S. Electrical energy storage systems: a comparative life cycle cost analysis. Renew Sustain Energy Rev 2015;42:569–96.
[14] Ogunjuyigbe AS, Ayodele TR, Akinola OA. Optimal allocation and sizing of PV/Wind/Split-diesel/Battery hybrid energy system for minimizing life cycle cost, carbon emission and dump energy of remote residential building. Appl Energy 2016;171(June):153–71.
[15] Salas V, Suponthana W, Salas RA. Overview of the off-grid photovoltaic diesel batteries systems with AC loads. Appl Energy 2015;157(November):195–216.
[16] Bhandari B, Lee KT, Lee CS, Song CK, Maskey RK, Ahn SH. A novel off-grid hybrid power system comprised of solar photovoltaic, wind, and hydro energy sources. Appl Energy 2014;133(November):236–42.
[17] Shang C, Srinivasan D, Reindl T. Generation-scheduling-coupled battery sizing of stand-alone hybrid power systems. Energy 2016;114(November):671–82.
[18] Fadaee M, Radzi MAM. Multi-objective optimization of a stand-alone hybrid renewable energy system by using evolutionary algorithms: a review. Renew Sustain Energy Rev 2012;16(5):3364–9.
[19] Nafeh AE. Optimal economical sizing of a PV-wind hybrid energy system using genetic algorithm. Int J Green Energy 2011;8(1):25–43.

[20] Kaabeche A, Belhamel M, Ibtiouen R. Sizing optimization of grid-independent hybrid photovoltaic/wind power generation system. Energy 2011;36 (2):1214–22.
[21] Li B, Roche R, Miraoui A. Microgrid sizing with combined evolutionary algorithm and MILP unit commitment. Appl Energy 2017;188 (February):547–62.
[22] Kaabeche Abdelhamid, Ibtiouen Rachid. Techno-economic optimization of hybrid photovoltaic/wind/diesel/battery generation in a stand-alone power system. Solar Energy 2014;103:171–82.
[23] Maleki Akbar, Askarzadeh Alireza. Optimal sizing of a PV/wind/diesel system with battery storage for electrification to an off-grid remote region: a case study of Rafsanjan, Iran. Sustain Energy Technol Assess 2014;7:147–53.
[24] Mukhtaruddin RNSR et al. Optimal hybrid renewable energy design in autonomous system using Iterative-Pareto-Fuzzy technique. Int J Elect Power Energy Syst 2015;64:242–9.
[25] Heydari A, Askarzadeh A. Optimization of a biomass-based photovoltaic power plant for an off-grid application subject to loss of power supply probability concept. Appl Energy 2016;165(March):601–11.
[26] Torsten Broeer et al. Modeling framework and validation of a smart grid and demand response system for wind power integration. Appl Energy 2014;113:199–207.
[27] Joung Manho, Kim Jinho. Assessing demand response and smart metering impacts on long-term electricity market prices and system reliability. Appl Energy 2013;101:441–8.
[28] Shen Bo et al. The role of regulatory reforms, market changes, and technology development to make demand response a viable resource in meeting energy challenges. Appl Energy 2014;130:814–23.
[29] Missaoui Rim et al. Managing energy smart homes according to energy prices: analysis of a building energy management system. Energy Build 2014;71:155–67.
[30] Wang X, Palazoglu A, El-Farra NH. Operational optimization and demand response of hybrid renewable energy systems. Appl Energy 2015;143 (April):324–35.
[31] Kernan R, Liu X, McLoone S, Fox B. Demand side management of an urban water supply using wholesale electricity price. Appl Energy 2017;189 (March):395–402.
[32] Nolan S, O'Malley M. Challenges and barriers to demand response deployment and evaluation. Appl Energy 2015;152(August):1.
[33] Menke R, Abraham E, Parpas P, Stoianov I. Demonstrating demand response from water distribution system through pump scheduling. Appl Energy 2016;170(May):377–87.
[34] Behboodi S, Chassin DP, Djilali N, Crawford C. Interconnection-wide hour-ahead scheduling in the presence of intermittent renewables and demand response: a surplus maximizing approach. Appl Energy 2017;189 (March):336–51.
[35] Babonneau F, Caramanis M, Haurie A. A linear programming model for power distribution with demand response and variable renewable energy. Appl Energy 2016;181(November):83–95.
[36] Tsui Kai Man, Chan Shing-Chow. Demand response optimization for smart home scheduling under real-time pricing. IEEE Trans Smart Grid 2012;3 (4):1812–21.
[37] Li Xiao Hui, Hong Seung Ho. User-expected price-based demand response algorithm for a home-to-grid system. Energy 2014;64:437–49.
[38] Yin R, Kara EC, Li Y, DeForest N, Wang K, Yong T, et al. Quantifying flexibility of commercial and residential loads for demand response using setpoint changes. Appl Energy 2016;177(September):149–64.
[39] Wang G, Zhang Q, Li H, McLellan BC, Chen S, Li Y, et al. Study on the promotion impact of demand response on distributed PV penetration by using non-cooperative game theoretical analysis. Appl Energy 2017;185 (January):1869–78.
[40] Lan Hai, Wen Shuli, Hong Ying-Yi, Yu David C, Zhang Lijun. Optimal sizing of hybrid PV/diesel/battery in ship power system. Appl Energy 2015;158:26–34.
[41] Tito SR, Lie TT, Anderson TN. Optimal sizing of a wind-photovoltaic-battery hybrid renewable energy system considering socio-demographic factors. Solar Energy 2016;136:525–32.
[42] Deshmukh SS, Boehm RF. Review of modeling details related to renewably powered hydrogen systems. Renew Sustain Energy Rev 2008;12(9):2301–30.
[43] Baghaee HR, Mirsalim M, Gharehpetian GB, Talebi HA. Reliability/cost-based multi-objective Pareto optimal design of stand-alone wind/PV/FC generation microgrid system. Energy 2016;115(November):1022–41.
[44] Hosseinalizadeh R, Shakouri H, Amalnick MS, Taghipour P. Economic sizing of a hybrid (PV–WT–FC) renewable energy system (HRES) for stand-alone usages by an optimization-simulation model: case study of Iran. Renew Sustain Energy Rev 2016;54(February):139–50.
[45] Celik Ali Naci. Energy output estimation for small-scale wind power generators using Weibull-representative wind data. J Wind Eng Indust Aerodyn 2003;91(5):693–707.
[46] Jahanshahloo GR, Hosseinzadeh F, Shoja N, Tohidi G. A method for solving 0–1 multiple objective linear programming problem using DEA. J Oper Res Soc Japan 2003;46(2):189–202.
[47] Kaldellis JK. The wind potential impact on the maximum wind energy penetration in autonomous electrical grids. Renewable Energy 2008;33 (7):1665–77.
[48] Iran Renewable Energy Organization (SUNA) Available At: <http://www.suna.org.ir/fa/home>.
[49] NASA Surface meteorology and Solar Energy-Location Available At: <https://eosweb.larc.nasa.gov>.
[50] Eltamaly AM, Mohamed MA, Alolah AI. A novel smart grid theory for optimal sizing of hybrid renewable energy systems. Solar Energy 2016;124 (February):26–38.
[51] Tabar VS, Jirdehi MA, Hemmati R. Energy management in microgrid based on the multi objective stochastic programming incorporating portable renewable energy resource as demand response option. Energy 2016(November).
[52] GAMS User Guide Available At: <http://www.GAMS.com>.
[53] HOMER® Pro Version 3.7 User Manual Available At: <www.homerenergy.com>.